


RESEARCH

Open Access



# Can non-contrast magnetic resonance imaging replace contrast-enhanced computerized tomography in the local staging of pediatric renal tumors?

Marwa Romeih<sup>1\*</sup> , Mary Rabea Mahrous<sup>2</sup>, Tarek Ahmed Raafat<sup>3</sup> and Esmat Mahmoud<sup>3</sup>

## Abstract

**Background** Renal tumors account for approximately 6–7% of the total incidence of pediatric cancers. Wilms tumor (WT) is the most common renal malignancy observed in the pediatric population under 5 years old. Computed tomography (CT) is used for staging of the renal tumors. Magnetic resonance imaging (MRI) offers enhanced soft tissue resolution and provides more comprehensive insights into tumor extension through the capsule, including tumor infiltration into the renal vein or IVC. MRI is a noninvasive imaging modality that does not involve any radiation hazards, making it safe for children. In addition, MRI can be performed without the administration of contrast agents in patients with impaired renal function. Therefore, MRI plays a vital role in screening, staging, preoperative evaluation, and follow-up. Diffusion-weighted imaging (DWI) is a functional tool that aids in locating the most receptive tumoral region to guide confirmatory biopsies. In this study, we aim to evaluate the potential value of non-contrast MRI in staging pediatric renal tumors compared to contrast-enhanced CT.

**Results** This study included 50 patients presented with renal mass, with ages ranging from 1 to 8 years and a mean age of  $4.27 \pm 1.27$  (mean  $\pm$  SD). The final diagnosis was Wilm's tumor at 86%, clear cell sarcoma at 4%, rhabdoid tumor at 4%, rhabdomyosarcoma at 2%, and nephroblastomatosis with no malignant transformation at 4%. CT accurately diagnosed stages 4 and 5 in agreement with pathological findings while upstaging the other cases, with a CT sensitivity of 90.91%, specificity of 82.35%, PPV of 92%, and NPV of 84%. MRI is superior to CT in stages 1 and 3, accurately diagnosing stages 2, 4, and 5, with a sensitivity of 93.30%, specificity of 95.65%, PPV of 95%, and NPV of 97%.

**Conclusions** Non-contrast MRI could be considered the optimal radiation-free imaging modality in staging pediatric renal tumors mainly Wilm's tumor as it offers high sensitivity and specificity of capsular and vascular infiltration, compared to contrast-enhanced CT especially in cases with impaired renal functions.

**Keywords** MR ICT, Staging pediatric renal tumors

## Background

Renal tumors comprise approximately 6–7% of all pediatric cancer cases. Wilms tumor (WT) is the most common renal malignancy observed in the pediatric population aged under 5 years. Renal cell carcinoma, clear cell sarcoma, and rhabdoid tumors have lower incidence rates, whereas leukemia and lymphoma have the lowest incidence rates [1, 2].

\*Correspondence:

Marwa Romeih

marwaromeih@gmail.com; marwa.romeih@med.helwan.edu.eg

<sup>1</sup> Radio-Diagnosis Department, Faculty of Medicine, Helwan University, Cairo, Egypt

<sup>2</sup> Radio-Diagnosis Department, National Heart Institute, Cairo, Egypt

<sup>3</sup> Radio-Diagnosis Department, National Cancer Institute, Cairo University, Cairo, Egypt

Nephroblastomatosis is a premalignant condition that affects children within their first year of life. It is characterized by multifocal involvement of the renal parenchyma. Wilm's tumor is frequently found in 90–100% of cases of bilateral nephroblastomatosis [3].

Renal tumor staging is essential for treatment planning and predicting outcomes. Contrast-enhanced CT (CECT) is the most frequently used modality for the assessment of renal tumors. Due to its availability, rapid scanning time, and capacity to assess the presence of pulmonary metastases simultaneously [4, 5].

MRI can accurately assess the renal tumor's extent through the capsule and its infiltration into the renal vein or IVC. This imaging modality poses no radiation risks, making it more suitable for pediatric patients. Furthermore, it can be performed without contrast in patients with impaired renal function [5, 6].

Therefore, MRI surpasses CT in the assessment and follow-up of pediatric renal masses [7]. It can also serve as an alternative for CT in local staging and pre-therapeutic assessment of renal tumors [8].

The utilization of a diffusion-weighted imaging (DWI) sequence and apparent diffusion coefficient (ADC) mapping can serve as noninvasive biomarkers with functional value. These biomarkers utilize differences in the diffusion of water molecules in tissues to deduce image contrast. It aids in locating the most receptive tumoral region to guide confirmatory biopsies [8, 9]. In our study, we aim to evaluate the potential value of non-contrast MRI in staging pediatric renal tumors compared to CECT.

## Methods

The Institutional Review Board approved the study. The patients' parents signed a written consent to use the clinical data in this study as our institute policy.

### Study population

This retrospective study aimed to evaluate pediatric patients referred to our hospital's Radiology Department. The study enrolled patients with suspected malignant renal masses previously identified by abdominal ultrasound (US) to evaluate and stage these masses accurately. The study was conducted between October 2019 and February 2022.

Inclusion criteria: Age  $\leq 18$  years, patients with renal masses were diagnosed using prior ultrasound (US). These individuals underwent both CECT and MRI, with 1 week or less interval between the CT and MRI examinations. Additionally, it was necessary to have access to pathology reports for the renal masses.

The exclusion criteria for this study included non-available pathology data and /or both CT and MRI examinations for the same patients.

## Data collection

### CT protocol and imaging data acquisition

All patients underwent CT examination using a sixty-four-section multi-detector CT (MDCT) scanner (Aquilion, Toshiba Medical Systems, Japan). Scans were performed before and after administration of intravenous non-ionic iodinated contrast media of 1.5 ml/kg body weight (Omnipaque 300) mg/ml, GE Healthcare, USA). The scans were obtained at 120 kV and 70–90 mAs/slice. Axial, coronal, and sagittal images were viewed at 3 to 5 mm slice thickness with a reconstruction interval of 1.5 mm. The estimated examination time was approximately 2–3 min.

### MR imaging

The MRI examination was performed using a magnetic resonance system (Achieva 1.5T, Phillips Medical Systems, The Netherlands) with a body/surface phased array coil.

For renal morphology assessment, axial T2 weighted fast spin-echo/ T2-weighted SPAIR (spectral Attenuated inversion recovery) and T1-weighted dual-echo in-phase and out-of-phase sequences, and coronal T2 weighted fast spin-echo.

Respiratory triggering axial DWI was obtained utilizing a single-shot spin echo planar with three  $b$  values of 0, 300, and 600  $s/mm^2$ . ADC maps were automatically generated, and ADC values were expressed in  $s/mm^2$ .

For each lesion, three regions of interest (ROIs) were measured in ADCs at 300 and 600  $s/mm^2$ . The ROIs did not include necrotic tissue or lesion margins. The minimum value was recorded for each  $b$  value among the three measurements. For each value of  $b$ , the minimum measurement was recorded. The ADC values were measured in the normal renal parenchyma of both kidneys, and ROIs were positioned in the central region of each kidney. The mean ADC values and standard deviation (SD) were calculated for each ROI.

A total of twenty-three children, all under the age of six, underwent sedation to obtain high-quality MRI images. The estimated examination time was 15–20 min.

### Image analysis, interpretation from CECT, and non-contrast MRI

Two expert radiology consultants with 15 and 17 years of expertise independently analyzed the CECT and MRI images. Both consultants were blinded to the pathological results. In case of disagreement, a third qualified radiologist with 25 years of experience was consulted to make the final decision. There was good inter-observer agreement.

Every renal lesion was assessed as follows:

- Mass size, location, and number.
- Tumor confined to kidney or extra-renal extension or capsule penetration:
  - Capsular penetration was considered positive if there was a focal protrusion in the mass and negative if the margin was well-defined and smooth.
- Tissue composition based on CT densities and MR signal characteristics (e.g., cystic, solid, hemorrhagic/proteinaceous, ossified).
- MR diffusion signal (restricted/facilitated) and measurement of ADC.
- Contrast enhancement (pattern and intensity).
- The presence of additional lesions in ipsilateral and contralateral kidneys
  - Contralateral synchronous lesions were considered positive if solid lesions were detected in the other kidney.
- Presence of renal vein or IVC invasion
  - Tumoral thrombus was considered if there was an extension of the tumor to the vessel or a discrete filling defect within it.
- The presence of lymph node (LN) metastasis
  - Positive LNs were defined as those with a short axis measuring 1 cm or more [10].
- The presence of intra-abdominal metastasis.
- The final classification of the renal tumor was documented as depicted in (Table 1) [11].
- In cases of nephroblastomatosis, as this is a pre-malignant renal condition, patients were evaluated for indications of malignant WT changes, such as focal heterogeneity of the lesions, altered density, or intensity [12].

#### Standard of references

The reference standard in our study was based on the surgical and pathological findings. The radiological staging

of CECT and MRI were compared with the histopathological post-surgical staging.

#### Statistical analysis

The SPSS software (version 12 for Windows) was used to analyze the data. The results were expressed as a mean  $\pm$  SD or percentage (%). The studied groups' CECT and MRI staging were compared using an unpaired *t* test. ANOVA test was utilized for mean comparison, whereas categorical data were compared using the Chi-square test. According to Galen's (1980) instructions, standard diagnostic indices such as sensitivity, specificity, positive predictive value (PPV), and negative predictive value (NPV) were computed. *P* values  $\leq 0.05$  were deemed significant, and *P* values  $\leq 0.01$  were considered highly statistically significant.

#### Results

The study included 50 child patients (30 males and 20 females). Patients' ages ranged from 1 to 8 years, with a mean of  $4.27 \pm 1.27$  (mean  $\pm$  SD). The clinical presentation was abdominal mass in 20 patients, hematuria in 12 patients, and abdominal mass and hematuria in 18 patients.

The lesion's size ranged from 3 to 14 cm with a mean of  $7.27 \pm 1.27$  (mean  $\pm$  SD). A total of 40% of the lesions originated from the left kidney, while 38% were from the right kidney. Bilateral lesions were observed in 22% of the cases.

The final diagnosis was Wilm's tumor ( $n=43$ ) 86%, clear cell sarcoma ( $n=2$ ) 4%, rhabdoid tumor ( $n=2$ ) 4%, rhabdomyosarcoma ( $n=1$ ) 2% and nephroblastomatosis with no malignant transformation ( $n=2$ ) 4%. The most common malignant lesions found in our study were Wilm's tumors, accounting for 86% of cases.

#### CT and MRI findings in correlation with pathology

The final pathological staging was as follows:

**Table 1** Wilm's tumor—clinic-pathological—National Wilm's Tumor Study (NWTS) staging [11]

Wilm's tumor—clinic-pathological—National Wilm's Tumor Study (NWTS) staging	
Stage I	Tumor confined to kidney without capsular or vascular invasion, tumor was not biopsied or ruptured. No residual tumor tissue after resection
Stage II	Tumor beyond renal capsule, vessel infiltration, biopsy performed before resection or intraoperative tumor rupture. Confined to the flank, not involving peritoneal surface (Completely resectable tumor with tumor-free margins)
Stage III	Tumor beyond renal capsule, vessel infiltration, biopsy performed before resection or intraoperative tumor rupture. Confined to the flank, not involving peritoneal surface (Completely resectable tumor with tumor-free margins)
Stage IV	Tumor beyond renal capsule, vessel infiltration, biopsy performed before resection or intraoperative tumor rupture. Confined to the flank, not involving peritoneal surface (Completely resectable tumor with tumor-free margins)
Stage V	Bilateral renal involvement present at diagnosis

- Two cases of nephroblastomatosis with no malignant transformation.
- Out of a total of 50 cases, 48 cases were as follows:

According to the data, 38% of cases were classified as stage I, whereas 6% were categorized as stage II. In addition, 26% of the cases were classified as stage III, whereas 10% were categorized as stage IV. Finally, 16% of the cases were categorized as stage V.

In relation to the staging performed by CT, 22% of the cases were diagnosed as stage I, 14% as stage II, 34% as stage III, 10% as stage IV, and 16% as stage V. The sensitivity of the staging was 90.91% with a 95% confidence interval (CI) of 75.67% to 98.08%, while the specificity was 82.35% with a 95% CI of 56.57% to 96.20%. PPV was 92%, and NPV was 84% (Fig. 1). The CT scan accurately identified stages 4 and 5 correlating with pathology while upstaging the other cases (Fig. 2).

Regarding the staging by MRI, 34% of the cases were diagnosed as stage I, 6% as stage II, 30% as stage III, 10% as stage IV, and 16% as stage V. The sensitivity of the MRI staging was 96.30%, with a 95% CI ranging from 81.03 to 99.91%. The specificity was 95.65%, with a 95% CI ranging from 78.05 to 99.89%. PPV was 95%, and NPV was

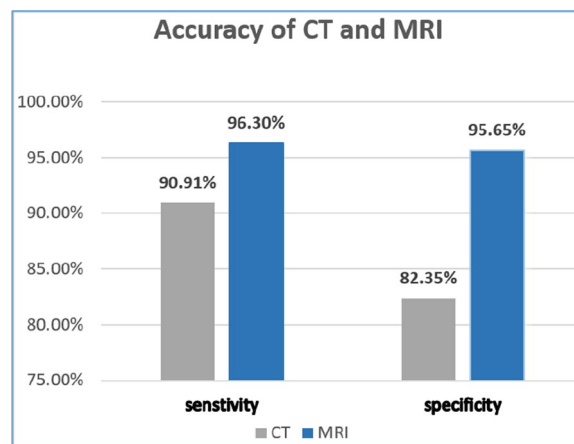


Fig. 2 Accuracy of CT and MRI

97% (Fig. 1). MRI accurately diagnosed stages 2, 4, and 5, surpassing the accuracy of CT in stages 1 and 3 (Fig. 2).

All the lesions showed diffusion restriction by qualitative (high signal at DWI), low ADC map, and quantitative values with ADC values ranging from 0.6 to  $1.1 \times 10^{-3} \text{ mm}^2/\text{s}$ . Diffusion restriction was significantly

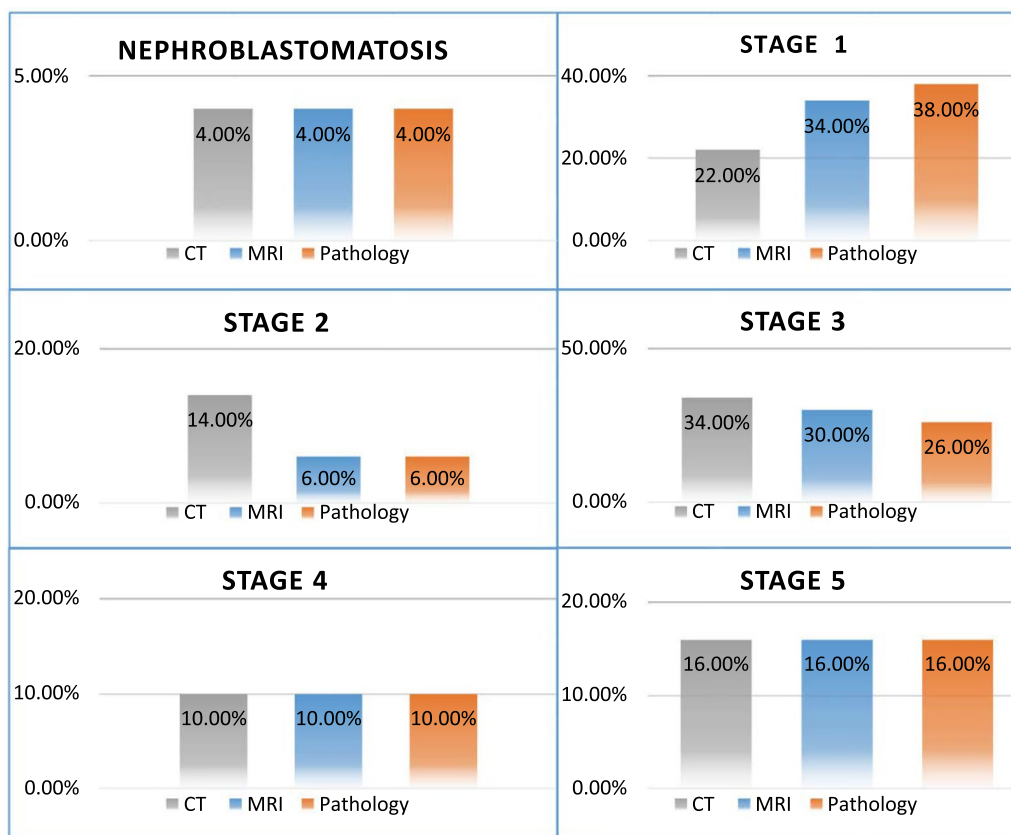


Fig. 1 Comparison between CT, MRI diagnosis and pathology

lower than normal parenchyma ADC. The central necrosis and hemorrhage areas demonstrated higher ADC values than the active areas (facilitated diffusion).

Regarding the capsular infiltration, MRI was more accurate than CT. Pathological analysis revealed capsular infiltration in 14 cases. MRI correctly detected capsular affection in cases. CT was positive in 17 cases, with false positive in three cases. Therefore, the CT showed over-staging of the cases as staging II in relation to the pathology (14% versus 6%, respectively) (Fig. 3).

The venous extension was positive in only 11/48 cases (6 renal veins, 5 IVC). CT accurately identified the venous extension in 85.4% of cases, while MRI achieved an accuracy rate of 89%, as demonstrated in (Fig. 4).

Lymph node metastasis was pathologically positive in 41.6% of cases (20/48). CT detected enlarged lymph nodes in 75% (15/20), while MRI detected positive lymph nodes in 80% of cases (16/20) (Fig. 5) (Table 2).

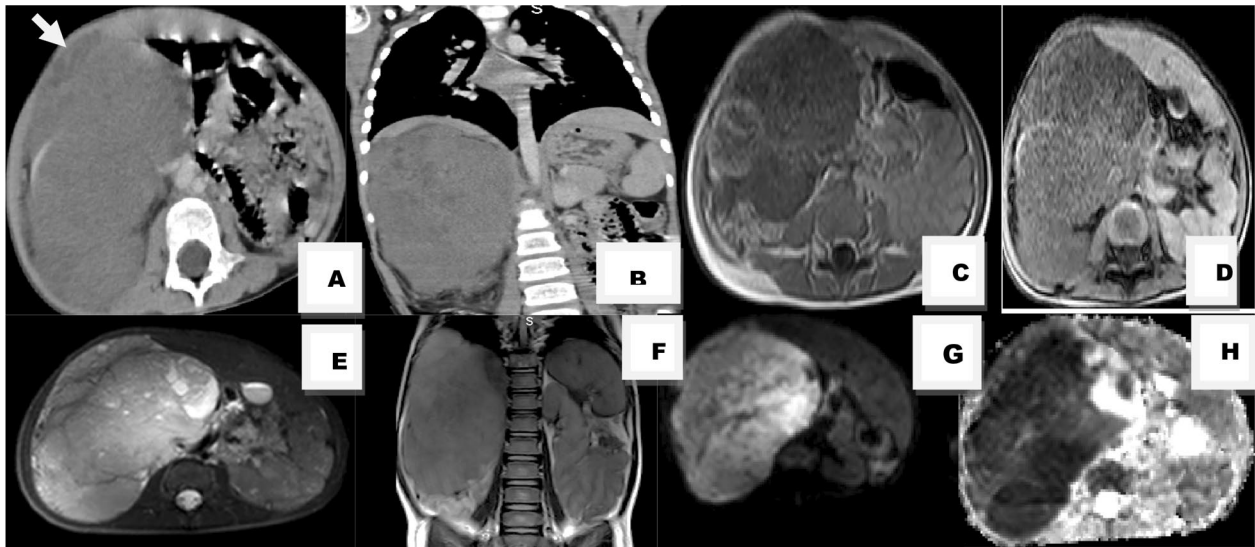


**Fig. 3** CECT **A, B** large right renal mass with capsular rupture (arrow). MRI **C, D** axial T1 out phase and in phase, respectively, **E** axial T2, **F** coronal T1 revealed intact renal capsule around the lesion, **G** Diffusion images with b values 600 show restricted diffusion of the mass lesion, with ADC value (**H**)  $0.8 \times 10^{-3} \text{ mm}^2/\text{s}$ . Pathology confirmed the diagnosis of the right Wilms tumor with an intact capsule (stage 1)

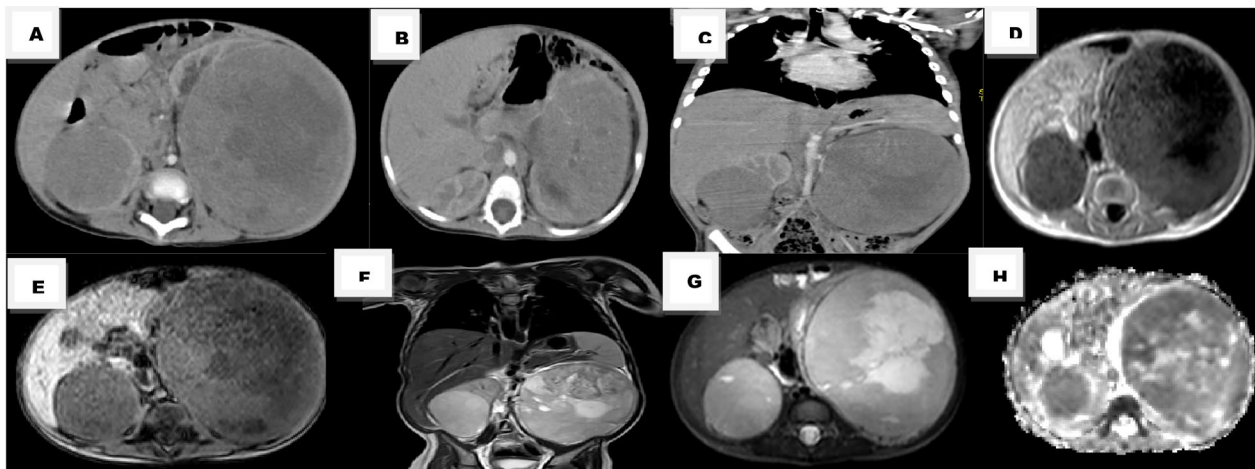


**Fig. 4** CECT **A–C** bilateral renal mass lesions, non-opacified IVC likely filling defect/thrombosis. MRI images **D, E** axial T1 out phase and in phase, respectively. **F** coronal T2 revealed bilateral mass lesions with normal signal void of the IVC with no evidence of thrombosis, **G** diffusion images with b values 600 showed diffusion restriction of both lesions, confirmed by low signals at ADC map, **H** with ADC value 0.8 at the right and  $0.5 \times 10^{-3} \text{ mm}^2/\text{s}$  at the left side. Pathology confirmed the diagnosis of bilateral Wilms with no vascular invasion (stage 5)

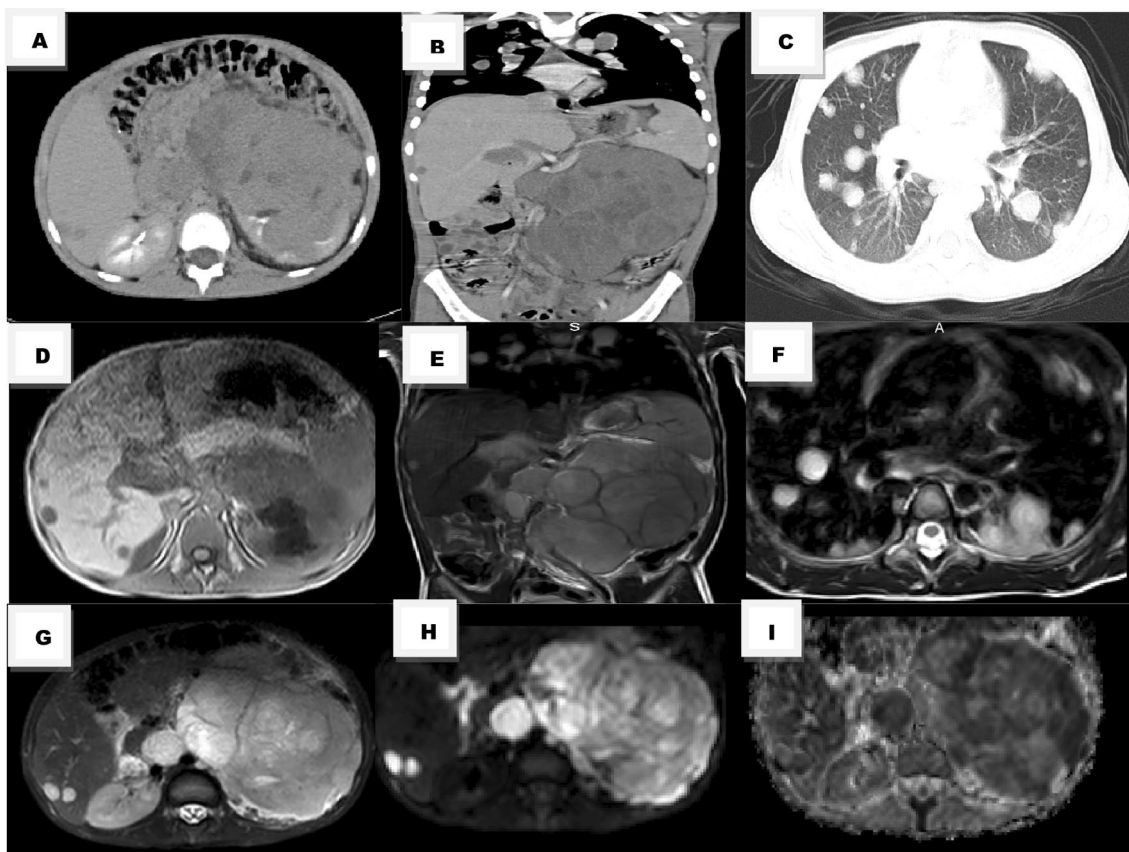


**Fig. 5** CECT **A–C** revealed a large left renal mass lesion, associated with large Aortocaval LN, hepatic focal lesions and multiple metastatic pulmonary nodules. MRI **D, E** T1 out phase and in phase, respectively, revealed a large left renal mass lesion, Aortocaval LN, hepatic focal lesions and **F** basal lung cuts revealed multiple metastatic pulmonary nodules, **G, H** diffusion images with *b* values 300 and 600 showed diffusion restriction of the renal lesion, LN as well as the hepatic focal lesions, confirmed by low signal at ADC map, **I** with ADC values ranging from 0.7 to  $0.9 \times 10^{-3} \text{mm}^2/\text{s}$ . Histopathology confirmed the diagnosis of the left Wilms tumor with distant metastasis (stage 4)

**Table 2** Capsular, nodal and IVC infiltration by CT, MRI and pathological finding

	CT	MRI	Pathology
Capsular infiltration	17	14	14/48
LN	15	16	20/48
Renal vein	4	5	6/48
IVC	5	5	5/48

Regarding bilateral lesions (Stage V), both CT and MRI correctly diagnosed all 16% of the pathologically proven synchronous bilateral lesions (Fig. 5).

**Nephroblastmatosis**

Our study included four cases of nephroblastmatosis identified through ultrasound examination. Suspected cases exhibited signs of malignant transformation. Two cases of nephroblastmatosis without malignant transformation

were identified using CT and MRI imaging techniques and confirmed by pathological examination. Additionally, two cases were found to have unilateral malignant transformation. Subsequent pathological examination confirmed that these cases were classified as (stage I) WT (Fig. 6).

**Diffusion and ADC map**

All the lesions exhibited diffusion restriction, as evidenced by qualitative (high signal at DWI), low ADC map, and quantitative values with ADC values ranging from  $0.6$  to  $1.1 \times 10^{-3} \text{mm}^2/\text{s}$ , which were significantly lower than normal parenchyma ADC. The central necrosis area showed higher ADC values than the active areas (facilitated diffusion).

Diffusion restriction was observed in cases of nephroblastmatosis, as indicated by the low ADC values ( $0.8 \times 10^{-3} \text{mm}^2/\text{s}$ ). Their high cellularity and condensed tissues make Brownian movement of water molecules

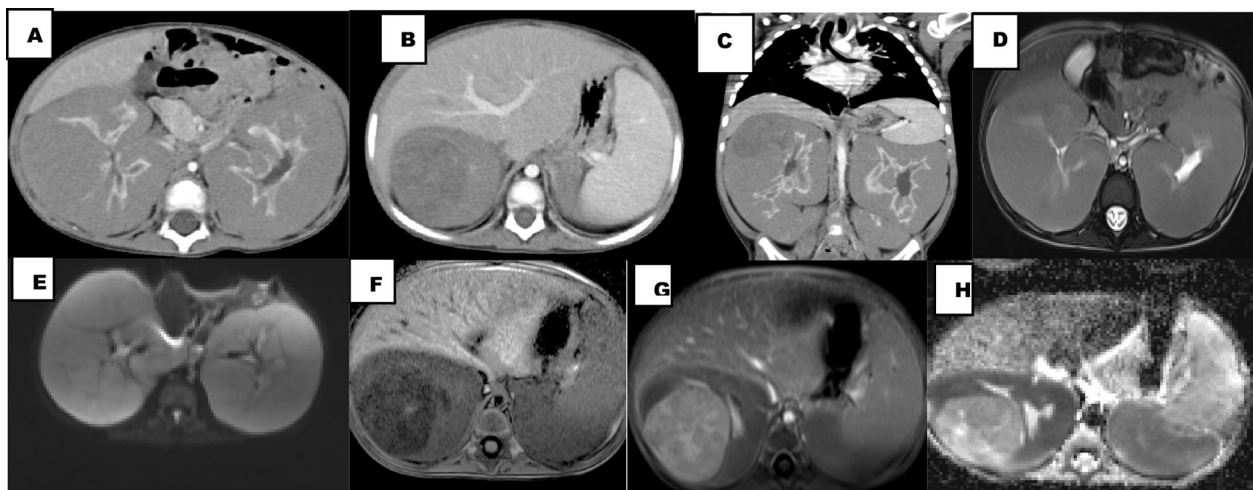


**Fig. 6** CECT **A–C** bilateral diffuse enlargement of the kidneys seen engulfed by hypodense cortical lesions denoting nephroblastomatosis with right focal heterogeneous lesion likely malignant transformation to Wilms with intact capsule. MRI images **D** axial T2 image revealed bilateral diffuse cortical low T2 engulfing renal parenchyma, **E** show diffuse restriction of both kidneys nephroblastomatosis, the right focal heterogeneous lesion, **F** low T1 with intact capsule, **G** diffusion images with  $b$  value 600 show restriction, **H** with ADC value  $0.5 \times 10^{-3} \text{ mm}^2/\text{s}$ . Histopathology confirmed the diagnosis of the right Wilms tumor on top of nephroblastomatosis (stage 1)

difficult, which is further supported by the lower ADC values than those of normal renal tissues.

## Discussion

The staging of pediatric renal tumors is crucial in treatment planning, whether it can be managed surgically or combined with chemo or radiotherapy [13]. CECT and MRI are two common diagnostic imaging modalities for accurately staging pediatric renal masses. However, MRI can provide a more accurate capsular and vascular infiltration assessment and comprehensive soft tissue characterization [14].

DWI is a sequence utilized to assess molecular diffusion. Tumor tissues have diffusion restriction due to the higher cellular tissue and increased index of neoplastic replication. Consequently, this reduces intercellular spaces and subsequent ultra-structural alteration of the kidney tissue [15].

In this study, we evaluated the value of non-contrast MRI in the staging of pediatric renal tumors in comparison to CECT.

The most common renal tumors observed were Wilms' tumor, accounting for 86% of cases, followed by clear cell sarcoma at 4%, rhabdoid tumor at 4%, rhabdomyosarcoma at 2%, and nephroblastomatosis without malignant transformation at 4%. These results are in agreement with the study conducted by Gee et al. [16], which revealed that Wilms' tumor accounts for 94% of pediatric renal tumors. Additionally, Anand et al. [17] found that 90% of these tumors were malignant, with Wilms' tumor

comprising 95% and other pathologies such as clear cell sarcoma, lymphoma, and rhabdoid tumor making up 5%.

CT demonstrated high accuracy in diagnosing stages 4 and 5, as confirmed by pathology while upstaging the other cases. CT sensitivity was 90.91%, while specificity was 82.35%. MRI accurately diagnosed stages 2, 4, and 5 and is more accurate compared to CT in stages 1 and 3. MRI sensitivity was 93.30%, while specificity was 95.65%, which aligns with Gee et al. [16]. They revealed that MRI is considered the imaging modality of choice for assessing multifocal disease and venous invasion, both of which have treatment implications. Furthermore, it is consistent with the findings of Meng et al. [5], who compared CT and MRI in staging renal tumors in children. The results demonstrated that CT has a sensitivity of 85% and a specificity of 82% in comparison to MRI, which has a sensitivity of 91% and specificity in the staging of pediatric renal tumors.

All cases in this study exhibited diffusion restriction, as evidenced by both qualitative and quantitative values, with ADC values ranging from  $0.6$  to  $1.1 \times 10^{-3} \text{ mm}^2/\text{s}$ . Diffusion restriction was significantly lower than normal parenchyma ADC. Diffusion showed false-positive results for nephroblastomatosis without malignant transformation, owing to their condensed tissues. Our results are consistent with a study by Platzer et al. [9], who illustrated that 11 patients were diagnosed with WT and six patients had nephroblastomatosis. All lesions had low mean ADC values  $< 1.0$ . Therefore, diffusion imaging and ADC values could not differentiate significantly between malignant disease and nephroblastomatosis. This can

be attributed to the high cellularity of the nephroblastomatosis that restricted diffusion. Kilickesmez et al. [18] demonstrated that diffusion can effectively differentiate between benign and malignant lesions. The average ADC values for malignant lesions ranged from  $(0.4 \text{ to } 1.08 \times 10^{-3} \text{ mm}^2/\text{s})$ .

The limitations of our study included the relatively limited number of cases examined, both in terms of the overall sample size and the number of cases for each pathological entity.

## Conclusions

Non-contrast MRI could be considered the optimal radiation-free imaging modality in staging pediatric renal tumors mainly Wilm's tumor as it offers high sensitivity and specificity of capsular and vascular infiltration, compared to contrast-enhanced CT especially in cases with impaired renal functions.

## Abbreviations

WT	Wilms tumor
CT	Computed tomography
CECT	Contrast-enhanced computed tomography
MRI	Magnetic resonance imaging
DWI	Diffusion-weighted imaging
ADC	Apparent diffusion coefficient

## Acknowledgements

NAD.

## Author contributions

All authors have read and approved the manuscript. MR formulated the research goals, participated in the research activity and responsible for correspondence to journal. MRM wrote the manuscript and collected patient data and was responsible for collection of patient's images. EM participated in the design of the study and performed the statistical analysis. ST conceived of the study and participated in its design and coordination, and was responsible for the review of the draft from a clinical point of view. TR assisted in data analysis, largely contributed in reviewing the manuscript and contributed in follow-up of the patients.

## Funding

This research did not receive any specific Grant from funding agencies in the public, commercial or not-for-profit sectors. There were no sources of funding.

## Availability of data and materials

The datasets used and/or analyzed during the current study are available from the corresponding author on reasonable request.

## Declarations

### Ethics approval and consent to participate

The study was approved by the Institutional Review Board (IRB) of the faculty of medicine, Helwan University, with ethical committee approval number 104-2023. Informed written consent was taken from all subjects.

### Consent for publication

Written informed consent from all patients' parents included in this research was obtained to publish the data contained within this study.

### Competing interests

The authors declare that they have no competing interests.

Received: 24 October 2023 Accepted: 13 January 2024

Published online: 22 January 2024

## References

- van der Beek JN, Watson TA, Nievelstein RAJ, Brisse HJ, Morosi C, Lederman HM et al (2022) MRI characteristics of pediatric renal tumors: a SIOP-RTSG radiology panel delphi study. *J Magn Reson Imaging* 55:543–552. <https://doi.org/10.1002/jmri.27878>
- Smets AM, De Kraker J (2010) Malignant tumours of the kidney: imaging strategy. *Pediatr Radiol* 40:1010–1018. <https://doi.org/10.1007/s00247-010-1584-z>
- Sandberg JK, Chi YY, Smith EA, Servaes S, Hoffer FA, Mullen EA et al (2020) Imaging characteristics of nephrogenic rests versus small Wilms tumors: a report from the Children's Oncology Group Study AREN03B2. *Am J Roentgenol*. <https://doi.org/10.2214/AJR.19.22301>
- Stanescu AL, Acharya PT, Lee EY, Phillips GS (2019) Pediatric renal neoplasms: MR imaging-based practical diagnostic approach. *Magn Reson Imaging Clin N Am* 27:279–290. <https://doi.org/10.1016/j.mric.2019.01.006>
- Meng J, Sun J (2022) Comparison of CT and MRI diagnostic performance in the abdominal staging of renal tumors in children. *Acta Medica Mediterr* 38:549–554. [https://doi.org/10.19193/0393-6384\\_2022\\_1\\_87](https://doi.org/10.19193/0393-6384_2022_1_87)
- Brisse HJ, Smets AM, Kaste SC, Owens CM (2008) Imaging in unilateral Wilms tumour. *Pediatr Radiol* 38:18–29. <https://doi.org/10.1007/s00247-007-0677-9>
- Artunduaga M, Eklund M, van der Beek JN, Hammer M, Littooi AS, Sandberg JK et al (2023) Imaging of pediatric renal tumors: a COG Diagnostic Imaging Committee/SPR Oncology Committee White Paper focused on Wilms tumor and nephrogenic rests. *Pediatr Blood Cancer* 70:4–9. <https://doi.org/10.1002/psc.30004>
- Wang ZJ, Westphalen AC, Zagoria RJ (2018) CT and MRI of small renal masses. *Br J Radiol*. <https://doi.org/10.1259/bjr.20180131>
- Platzer I, Li M, Winkler B, Schweinforth P, Pabst T, Bley T et al (2015) Detection and differentiation of paediatric renal tumours using diffusion-weighted imaging: an explorative retrospective study. *Cancer Res Front* 1:178–190. <https://doi.org/10.17980/2015.178>
- He L, Sun Y, Huang G (2021) Identifying threshold sizes for enlarged abdominal lymph nodes in different age ranges from about 200,000 individual's data. *Sci Rep* 11:1–7. <https://doi.org/10.1038/s41598-021-81339-9>
- Theilen TM, Braun Y, Bochennek K, Rolle U, Fiegel HC, Friedmacher F (2022) Multidisciplinary treatment strategies for Wilms tumor: recent advances, technical innovations and future directions. *Front Pediatr* 10:1–14. <https://doi.org/10.3389/fped.2022.852185>
- de Jesus LE, Fulgencio C, Leve TC, Dekermacher S (2022) Nephroblastomatosis and wilms tumor: dangerous liaisons. *Int Braz J Urol* 48:157–164. <https://doi.org/10.1590/S1677-5538.IBJU.2020.0694>
- Tselis N, Chatzikonstantinou G (2019) Treating the chameleon: radiotherapy in the management of renal cell cancer. *Clin Transl Radiat Oncol* 16:7–14. <https://doi.org/10.1016/j.ctro.2019.01.007>
- Bălănescu RN, Băetu AE, Moga AA, Bălănescu L (2022) Role of ultrasonography in the diagnosis of Wilms' tumour. *Children*. <https://doi.org/10.3390/children9081252>
- Hötter AM, Lollert A, Mazaheri Y, Müller S, Schenk JP, Mildnerberger PC et al (2020) Diffusion-weighted MRI in the assessment of nephroblastoma: results of a multi-center trial. *Abdom Radiol* 45:3202–3212. <https://doi.org/10.1007/s00261-020-02475-w>
- Gee MS, Bittman M, Epelman M, Vargas SO, Lee EY (2013) Magnetic resonance imaging of the pediatric kidney: benign and malignant masses. *Magn Reson Imaging Clin N Am* 21:697–715. <https://doi.org/10.1016/j.mric.2013.06.001>
- Anand R, Narula MK, Gupta I, Chaudhary V, Choudhury S, Jain M (2012) Imaging spectrum of primary malignant renal neoplasms in children. *Indian J Med Paediatr Oncol* 33:242–249. <https://doi.org/10.4103/0971-5851.107107>
- Kilickesmez O, Inci E, Atilla S, Tasdelen N, Yetimođlu B, Yencilek F et al (2009) Diffusion-weighted imaging of the renal and adrenal lesions. *J Comput Assist Tomogr* 33:828–833. <https://doi.org/10.1097/RCT.0b013e31819f1b83>

## Publisher's Note

Springer Nature remains neutral with regard to jurisdictional claims in published maps and institutional affiliations.